Research Article

Cancer Immunology Research

Apoptotic Cells Release IL1 Receptor Antagonist in Response to Genotoxic Stress

Jyh Yun Chwee[1,2], Muznah Khatoo[1], Nikki Yi Jie Tan[1], and Stephan Gasser[1,2]

Abstract

Apoptosis is a controlled means of eliminating damaged cells without causing an inflammatory response or tissue damage. The mechanisms that contribute to the suppression of an inflammatory response upon apoptosis of cells are poorly understood. Here, we report that apoptotic cells release the interleukin-1 receptor antagonist (IL1RA). The release of IL1RA depended on the DNA damage response, caspase 9, and caspase 3. *De novo* translation, classical secretion pathways, or N-glycosylation was not required for the release of IL1RA. The amounts of IL1RA released by apoptotic cells impaired IL1-induced expression of *IL6*. In summary, we demonstrate that the release of IL1RA in response to genotoxic stress contributes to the immunosuppressive effects of apoptotic cells. *Cancer Immunol Res; 4(4); 294–302. ©2016 AACR.*

Introduction

Cells are subjected to various genotoxic insults throughout their life cycle, resulting in DNA lesions that affect genomic DNA replication and transcription (1). If not repaired properly, DNA lesions can result in mutagenesis and wide-scale genomic aberrations that endanger the survival of the individual cell and the organism. Cells express sensor proteins that recognize DNA lesions and stalled replication forks (2). These sensor proteins initiate a DNA damage response (DDR), which imposes cell-cycle arrest, allowing DNA repair, or induces apoptosis if the DNA damage is too extensive to be repaired (3).

The regulated degradation of cell contents during apoptosis prevents the release of inflammatory intracellular factors (4, 5). Inflammatory responses are also suppressed by the release of anti-inflammatory mediators, such as IL10, TGFβ, and prostaglandins by macrophage, upon phagocytosis of apoptotic cells. However, the anti-inflammatory effects mediated by apoptotic cells are still not well understood.

IL1 is a critical cytokine in inflammation, innate immunity, angiogenesis, and hematopoiesis (6). IL1 is encoded by two genes, IL1α and IL1β, which induce the expression of proinflammatory factors such as IL6 upon binding to IL1 receptor type 1 (IL1R1; ref. 7). IL1α and IL1β are synthesized as precursor proteins that are processed into mature forms. Both the pro-IL1α and the mature IL1α forms are biologically active, whereas IL1β requires processing by caspase 1 (8). IL1α precursors are constitutively expressed in fibroblasts, epithelial cells, and keratinocytes. Upon apoptosis, IL1α is sequestered intracellularly, which prevents the promotion of inflammation (9).

The IL1RA competes with IL1 for binding to the IL1R1 and disrupts the proinflammatory signaling pathways (10). IL1RA exists as a secreted soluble IL1RA (sIL1Ra) isoform and three intracellular (icIL1RA) isoforms. The ratio of IL1RA to IL1 was found to be critical for the control of inflammatory responses in animal and patients studies (11–13). *IL1ra*-deficient mice exhibit excessive inflammation when bred to various disease models, and patients with *IL1RA* deficiency show severe inflammatory conditions (14–19). The icIL1RA isoforms are considered a reservoir of biologic active IL1RA, but the factors that regulate the release of icIL1RA have not been studied in detail (6, 20–23).

Here, we report that apoptosis in response to genotoxic stress results in the release of intracellular IL1RA, but not IL1α or IL1β. The release of IL1RA depended on ATM, caspase-9, and caspase-3 activation, but did not require *de novo* protein synthesis, classical secretion pathways, or N-glycosylation. IL1RA released in response to bleomycin treatment impaired IL1-induced *IL6* expression. In summary, we show that caspase-mediated apoptosis leads to the release of biologically active intracellular IL1RA.

Materials and Methods

Ethics statement

Mice were housed and bred in pathogen-free conditions in strict compliance with the Institutional Animal Care and Use Committee guidelines at the National University of Singapore, in accordance with the National Advisory Committee for Laboratory Animal Research guidelines (Guidelines on the Care and Use of Animals for Scientific Purposes). The protocol was approved by the Institutional Animal Care and Use Committee of the National University of Singapore (Protocol number: 041/08), and steps were taken to minimize suffering.

Mice

C57BL/6 mice were purchased from the Centre for Animal Resources at the National University of Singapore (Singapore). *IL1r*-deficient mice were obtained from the Jackson Laboratory. Ears derived from *IL1ra*-deficient mice were kindly provided by Dr. C. Wakabayashi (National Institute of Neuroscience, Japan).

[1]Immunology Programme and Department of Microbiology and Immunology, Centre for Life Sciences, National University of Singapore, Singapore. [2]National University of Singapore Graduate School for Integrative Sciences and Engineering, National University of Singapore, Singapore.

Corresponding Author: S. Gasser, Centre for Life Sciences, National University of Singapore, 28 Medical Drive, Singapore 117456, Singapore. Phone: 65167209; Fax: 67782684; E-mail: micsg@nus.edu.sg

doi: 10.1158/2326-6066.CIR-15-0083

AACR

Cells

Primary fibroblasts from adult C57BL/6 mice were established as previously described (24). Isolated fibroblasts were cultured in RPMI 1640 medium (Invitrogen) supplemented with 5% heat-inactivated FCS (Invitrogen), 150 μmol/L β-mercaptoethanol (Sigma), 1.4 μmol/L of L-glutamine (Sigma), 20 U/mL of penicillin–streptomycin (Invitrogen), and 20 mmol/L of HEPES (Hyclone) for 12 to 24 days before being used for experiments. The mouse monocytic leukemic macrophage cell lines RAW 264.7 (<10 passages) and J774.2 (<10 passages) were obtained from ATCC. The TRAMP-C2 prostate cancer cell line (<10 passages) was kindly provided by Dr. D.H. Raulet (University of California, Berkeley, CA). BC2 cells were a generous gift by Dr. Corcoran (Wehi, Australia; <20 passages). All cells were maintained at 37°C in a humidified 5% CO_2 incubator (Thermo Scientific).

Treatments

A total of 2.5×10^5 primary fibroblasts or RAW 264.7 cells were treated with 20 μg/mL of cycloheximide (Merck Millipore), 5 μg/mL of tunicamycin (Sigma), or 20 mmol/L of 2-Deoxy-D-glucose (Sigma) for 1 hour, followed by treatment with 30 μg/mL of bleomycin (Merck Millipore) or 0.5 μg/mL of doxorubicin (Santa Cruz technology) for 20 hours.

To investigate the role of secretory pathways, 2.5×10^5 primary fibroblasts were treated with 30 μg/mL of bleomycin (Merck Millipore) for 14 hours, followed by 1 μg/mL of BD GolgiStop (BD Biosciences) and 2 μmol/L of Protein Transport Inhibitor (BD Biosciences) for 6 hours.

To study the role of caspases, 2.5×10^5 primary fibroblasts were treated with 20 μmol/L of the pan-caspase inhibitor, Z-VAD-FMK (Santa Cruz Technology), 10 μmol/L of caspase-9

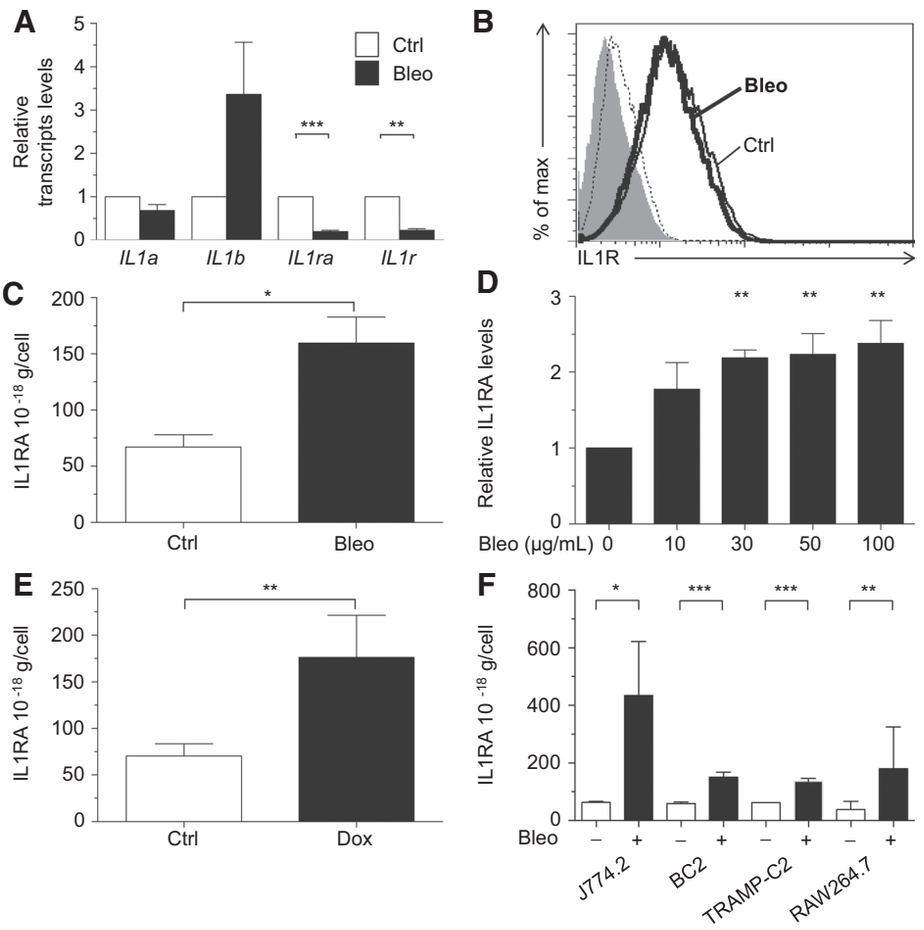

Figure 1.

Release of IL1RA in response to DNA damage. A, relative *IL1a, IL1b, IL1ra*, and *IL1r* transcript levels in primary fibroblasts treated with 30 μg/mL of bleomycin (bleo) for 20 hours were determined by qRT-PCR and compared with levels from control-treated cells. B, cell surface expression of IL1R in primary fibroblasts treated with bleomycin was analyzed by flow cytometry. IL1R expression of fibroblasts treated with 30 μg/mL of bleomycin for 20 hours (thick line) or vehicle control (thin line) was compared with isotype stained DMSO (filled histograms) or bleomycin-treated cells (dashed lines). One out of three representative experiments is shown. C, supernatant of primary fibroblasts treated with 30 μg/mL of bleomycin or with vehicle control was collected after 20 hours and analyzed for amounts of IL1RA by ELISA. D, supernatant of primary fibroblasts treated with the indicated doses of bleomycin for 20 hours was analyzed for amounts of IL1RA by ELISA and compared with the amounts of IL1RA present in vehicle-treated fibroblasts. E, supernatant of primary fibroblasts treated with 0.5 μg/mL doxorubicin or with vehicle control was collected after 20 hours and analyzed for amounts of IL1RA by ELISA. F, supernatant of macrophage-like J774.2 and RAW264.7 cancer cells, BC2 B-cell lymphoma cells, and TRAMP-C2 prostate cancer cells treated with 30 μg/mL of bleomycin or with vehicle control were collected after 20 hours and analyzed for amounts of IL1RA by ELISA. The results of experiments in A, C, and F are expressed as mean ± SE of at least three independent experiments. *, $P < 0.05$; **, $P < 0.01$; and ***, $P < 0.001$.

inhibitor, Z-LEHD-FMK (BD Biosciences), or 10 μmol/L of caspase-3 inhibitor, Z-DEVD-FMK (Santa Cruz Technology) for 1 hour, followed by treatment with 30 μg/mL of bleomycin (Merck Millipore) for 20 hours. Supernatant was harvested from each well, centrifuged at 1,500 rpm for 5 minutes at 4°C to remove cell debris, and stored at −80°C until analysis.

To investigate the role of the DDR, 2.5×10^5 primary fibroblasts were treated with 10 μmol/L of the ATM kinase-specific inhibitor, KU-60019 (R&D systems, USA) or 5 mmol/L of caffeine (Sigma, Singapore) for 1 hour, followed by treatment with 30 μg/ml of bleomycin (Merck Millipore) for 20 hours.

To assess bioactivity of IL1RA, primary fibroblasts were seeded at a density of 2.5×10^5 cells per well in 6-well dishes and treated with 30 μg/mL of bleomycin (Merck Millipore) for 20 hours. The supernatant was transferred to a second set of fibroblasts. One hour later, recombinant IL1α (Peprotech) at the indicated concentrations was added for 6 hours. Alternatively, the supernatant was transferred to J774.2 cells transfected with 1 μg/mL of poly (dA:dT) LyoVec (Invivogen) overnight after pretreatment with 1 μmol/L of PMA (Sigma) for 3 hours and subsequent treatment with 2 μg/mL of LPS for 16 hours. The levels of *IL6* transcripts were measured by real-time PCR.

Quantitative real-time PCR

The RNeasy Mini Kit (Qiagen) was used to isolate total RNA from treated cells. Reverse transcription was performed using 2 μg of total RNA, random hexamer primer, and moloney murine leukemia virus reverse transcriptase (M-MLV RT; Promega). For PCR, an amplification mixture consisting of 50 ng of reverse-transcribed RNA, 0.2 μmol/L forward primer, 0.2 μmol/L reverse primer, and 12.5 μL of iTaq SYBR Green Supermix with ROX (Biorad Laboratories) was prepared (25 μL). PCRs were performed in duplicates using the ABI PRISM 7700 Sequence Detection System from Applied Biosystems. The PCR thermocycling parameters were 50°C for 2 minutes, 95°C for 10 minutes, and 40 cycles of 95°C for 15 seconds and 60°C for 15 seconds and 72°C for 1 minute. All samples were normalized to their respective housekeeping gene hypoxanthine phosphoribosyltransferase (*Hprt*). The following primers were used: *Hprt*-5′, tgggaggccatcacattgt, *Hprt*-3′: gcttttccagtttcactaatgaca; *IL1α*-5′: gccagttgagtaggataaagg, *IL1α*-3′: cagtctgtctccttcttgagg; *IL1β*-5′: tcacagcagcacatcaacaa, *IL1β*-3′: tgtcctcatcctggaaggtc; *IL1ra*-5′: gggatactaaccagaagacc, *IL1ra*-3′: gacaggcacagcttgccccc; *sIL1ra*-5′: cttgctgtggcctcgggatgg, *sIL1ra*-3′: ctttttcccagaagggcggcagg; *icIL1ra*-5′: tccaccctgggaaggtctgtgc, *icIL1ra*-3′: gctgcctctgaagccatgggtg; and *IL6*-5′: tgcaagagacttccatccagttg, *IL6*-3′: cctccgacttgtgaagtggt. Samples without RNA were included as negative controls.

Flow cytometry

Phycoerythrin-conjugated antibody to IL1R1 was purchased from BD Pharmingen. Dead cells were excluded from the analysis based on the side scatter versus forward scatter profile, and based on exclusion of propidium iodide (Sigma) fluorescence signal. Intracellular staining of caspase 3 was performed using the BD intracellular fixation and permeabilization Kit (BD Biosciences) according to the manufacturer's instructions. Briefly, cells were stained with the viability dye eFluor 780 (eBioscience) at 4°C for 30 minutes. Data acquisition was performed on a FACSCalibur (BD Biosciences) or a CyAn ADP analyzer (Beckman Coulter) and analyzed using Flowjo software 8.8.7 (Tree Star Inc.).

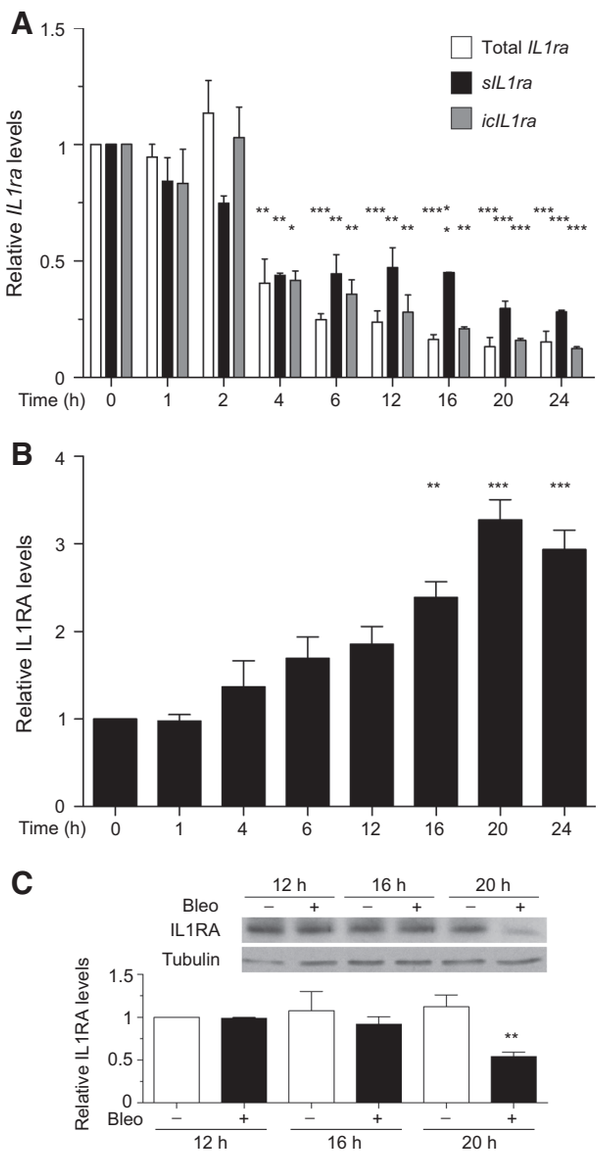

Figure 2.
IL1ra transcript levels decrease in response to DNA damage. A, relative transcript levels of total *IL1ra* (white column), secreted *IL1ra* (*sIL1ra*; black column), and intracellular *IL1ra* (*icIL1ra*; gray column) in primary fibroblasts treated with 30 μg/mL of bleomycin for the indicated periods of time were assessed by qRT-PCR. Transcript levels were normalized to vehicle-treated cells. B, concentrations of IL1RA in the supernatant of primary fibroblasts treated with 30 μg/mL of bleomycin for the indicated periods of time were analyzed by ELISA and compared with concentrations in control-treated cells. Results are expressed as mean ± SE of at least three independent experiments. C, immunoblot analysis of fibroblasts treated with 30 μg/mL of bleomycin for the indicated hours. Immunoblots were probed with antibodies specific for IL1RA and tubulin (top). Densitometry analysis of immunoblots showing mean ± SD from three experiments normalized to tubulin levels (bottom). *, $P < 0.05$; **, $P < 0.01$; ***, $P < 0.001$.

Apoptotic cells were detected using the Annexin V apoptosis detection Kit (eBioscience) according to the manufacturer's guidelines.

Western blotting

For the preparation of whole-cell extracts, cells were lysed in RIPA buffer consisting of 150 mmol/L NaCl, 1 mmol/L EDTA, 50 mmol/L Tris-HCl (pH 7.4), 1% NP-40, and 1% sodium deoxycholate (Sigma). The protease inhibitor cocktail set III and phosphatase inhibitor cocktail set V (Merck Millipore) were added to the lysis buffer according to the manufacturer's instructions prior to cell lysis. The whole-cell extracts were electrophoresed in 12% sodium dodecyl sulfate polyacrylamide gels and blotted onto nitrocellulose membranes (Amersham). The membranes were probed with the following antibodies: IL1RA/IL1F3 MAb (Clone 694204; RnD Systems) followed by Horseradish peroxidase (HRP)–conjugated goat anti-mouse or anti-rabbit IgG (Jackson Immunoresearch). GAPDH expression was detected with a GAPDH antibody conjugated to HRP purchased from Sigma.

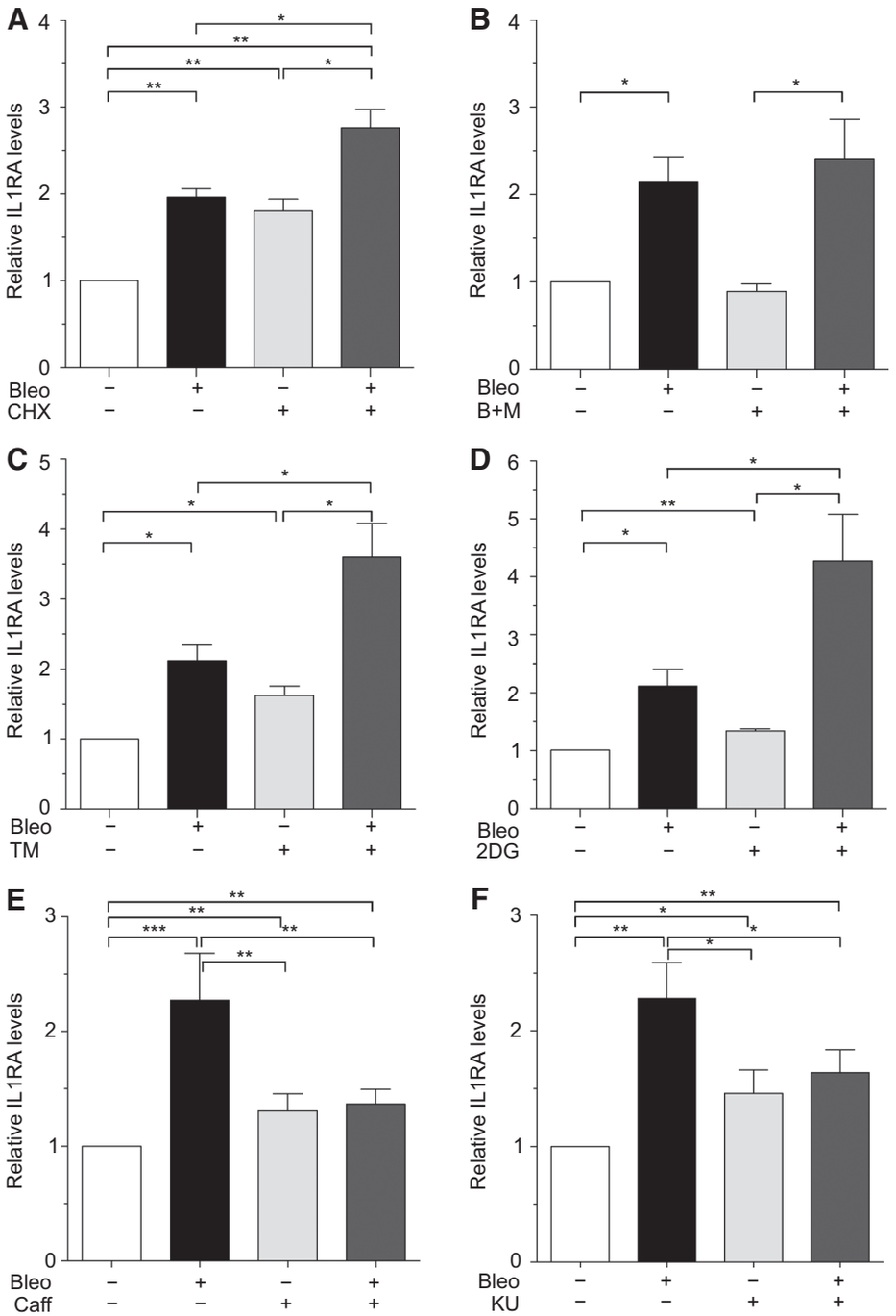

Figure 3.
Release of IL1RA in response to DNA damage does not depend on *de novo* translation or classical secretory pathways. A, primary fibroblasts were pretreated for 1 hour with 20 μg/mL of the translational inhibitor cycloheximide (CHX) followed by treatment with 30 μg/mL of bleomycin or vehicle control for 20 hours. Supernatant of treated cells was collected and analyzed for IL1RA levels by ELISA. The amounts of IL1RA were compared with those from the vehicle-treated group. B, primary fibroblasts were treated with 30 μg/mL of bleomycin or vehicle for 20 hours. During the last 6 hours of treatment, the protein secretion inhibitors Brefeldin A (B, 1 μg/mL) and monensin (M, 2 μmol/L) were added, and the supernatant was analyzed for the amounts of IL1RA by ELISA. The levels of IL1RA were compared with levels from vehicle-treated cells. C and D, cells were treated as described in A, but 5 μg/mL of the N-glycosylation inhibitors tunicamycin (TM; C) or 20 mmol/L of 2-Deoxy-D-glucose (2DG; D) were added instead of CHX. E and F, cells were treated as described in A, but pretreated for 1 hour with 5 mmol/L of caffeine (Caff; E) or 10 μmol/L of the ATM kinase–specific inhibitor, KU-60019 (KU). Results of all experiments are expressed as mean ± SE of four independent experiments. *, $P < 0.05$; **, $P < 0.01$; ***, $P < 0.001$.

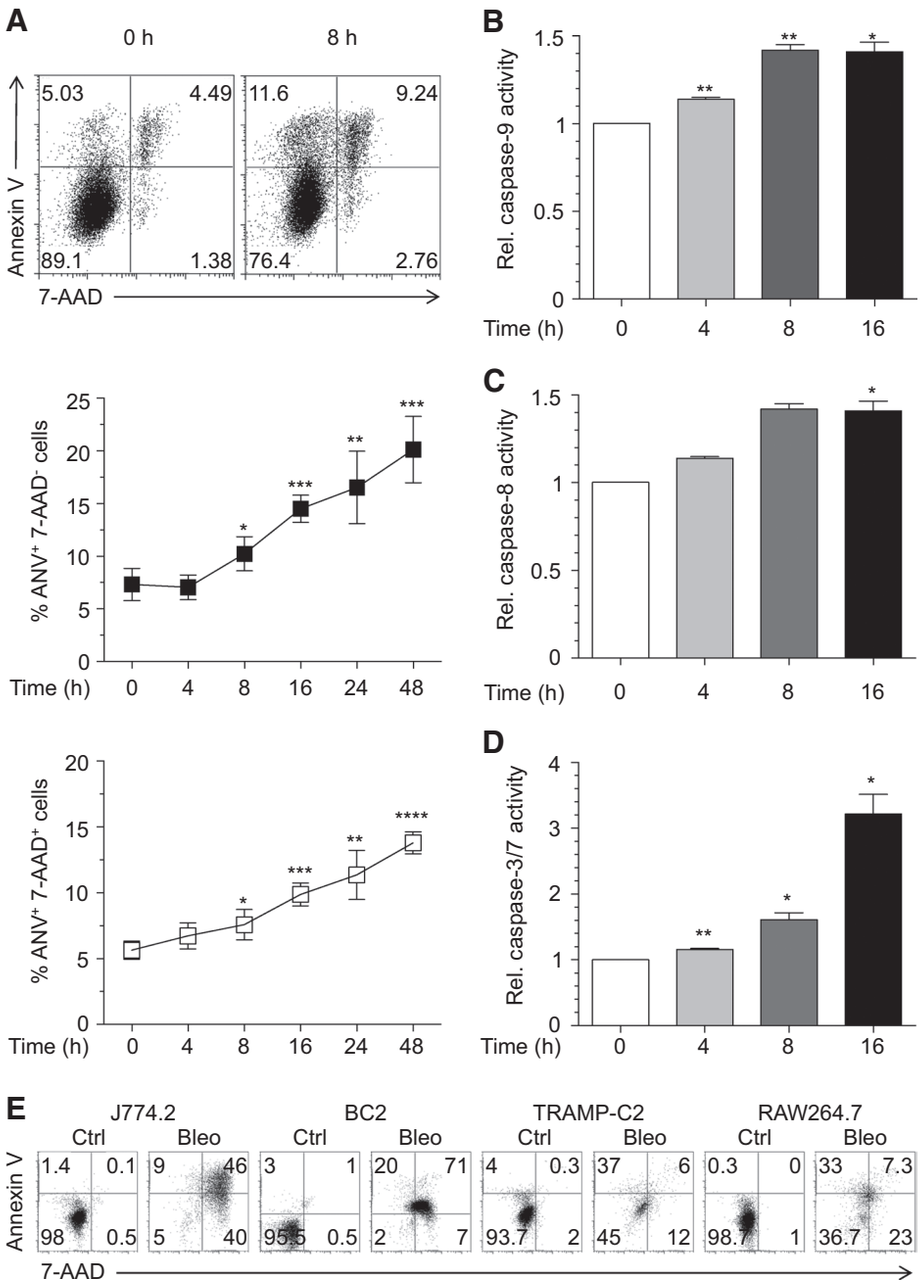

Figure 4.
Bleomycin induces apoptosis of fibroblasts and cancer cells. A, primary fibroblasts treated with 30 μg/mL of bleomycin or vehicle control for the indicated time were assessed for apoptosis by staining for 7-AAD and Annexin V (ANV) by flow cytometry. A representative dot plot of Annexin V and 7-AAD staining at 0 and 8 hours of treatment is shown in the top plot. Annexin V^+ 7-AAD^- (filled squares in the middle) and Annexin V^+ 7-AAD^+ (open circles in the bottom) cells were considered apoptotic. B–D, primary fibroblasts were treated with 30 μg/mL of bleomycin for the indicated periods of time and analyzed for caspase-9 (B), caspase-8 (C), and caspase-3/7 (D) activities using Caspase-Glo assays. Caspase activity was normalized to untreated cells. The results are expressed as mean ± SE of three independent experiments. E, J774.2, BC2, TRAMP-C2, and RAW267.7 cells were treated and analyzed as described in A. *, $P < 0.05$; **, $P < 0.01$; ***, $P < 0.001$; ****, $P < 0.0001$.

ELISA

The quantification of IL1α and IL1RA was determined using ELISA kits from R&D Systems. Quantification of IL1β and IL6 was determined using ELISA Ready Set Go kits (eBioscience) according to the manufacturer's instructions.

Caspase assays

Caspase-Glo assays (Promega) were used to measure caspase-3/7, -8, and -9 activities as instructed by the manufacturer. Primary fibroblasts were seeded at a density of 2×10^4 to 4×10^4 cells/well of a 96-well plate and treated as indicated. Luminescent signals were analyzed using a Wallac 1420 VICTOR2 (Perkin Elmer).

Statistical analyses

Statistical analyses were performed using the Student *t* test in Prism 6.0f (Graphpad). Error bars denote ±SD. *, $P < 0.05$; **, $P < 0.01$; ***, $P < 0.001$; and ****, $P < 0.0001$.

Results

Release of IL1RA by fibroblasts in response to DNA damage

The expression of IL1α and IL1β is increased in response to persistent DNA damage (25). To assess the effects of acute DNA damage on IL1 family members, we treated primary murine fibroblasts derived from adult tail and ear tissue with the radiomimetic bleomycin for 20 hours. Acute DNA

damage in response to bleomycin failed to significantly increase *IL1a* and *IL1b* transcripts levels (Fig. 1A). In contrast, bleomycin treatment decreased *IL1r* ($P < 0.002$) and *IL1ra* ($P < 0.001$) transcripts. The presence of fewer *IL1a* and *IL1b* transcripts differentially affected protein amounts. The IL1R expression at the cell surface did not significantly change during bleomycin treatment of cells (Fig. 1B). In contrast, the amounts of IL1RA increased in the supernatant of bleomycin-treated cells in a dose-dependent manner (Fig. 1C and D; $P < 0.05$). Treatment of fibroblasts with doxorubicin, a genotoxic topoisomerase II inhibitor, also induced the release of IL1RA ($P < 0.005$), suggesting that IL1RA is released by fibroblasts in response to acute DNA damage (Fig. 1E). The release of IL1RA was not limited to fibroblasts as B-cell lymphoma, prostate cancer cells, and macrophage-like cancer cells also released IL1RA in response to bleomycin (Fig. 1F and data not shown).

A closer analysis of *Il1ra* and IL1RA transcript levels showed that secreted (*sIL1ra*) and intracellular (*icIL1ra*) *Il1ra* transcripts decreased within 4 hours (Fig. 2A). In contrast, the amounts of IL1RA gradually increased in the supernatant of bleomycin-treated fibroblasts after 16 hours, indicating that bleomycin-induced release of IL1RA is independent of transcription (Fig. 2B; $P < 0.01$). The increase of IL1RA in the supernatant was in contrast with reduced intracellular IL1RA 20 hours after bleomycin treatment (Fig. 2C; $P < 0.01$). Hence, our data indicate that the intracellular pool of IL1RA is released in response to DNA damage.

Release of IL1RA is independent of *de novo* translation and secretion

To test if bleomycin-induced IL1RA secretion requires *de novo* protein synthesis, we inhibited protein translation with cycloheximide. Pretreatment of fibroblasts with cycloheximide did not abrogate bleomycin-induced IL1RA levels (Fig. 3A; $P < 0.004$). Interestingly, cycloheximide also induced the release of IL1RA, and the effects of cycloheximide and bleomycin were additive (Fig. 3A; $P < 0.002$).

Next, we analyzed if the release of IL1RA depended on secretion via the endoplasmic reticulum (ER)–Golgi complex secretory pathway. The release of IL1RA was not significantly impaired by the addition, during the last 6 hours of bleomycin treatment, of brefeldin A and monensin, which disrupt the ER–Golgi complex secretory pathway (Fig. 3B).

N-glycosylation regulates the secretion and degradation of certain proteins (26). Inhibition of N-glycosylation by tunicamycin or 2-deoxy-D-glucose did not hamper the release of IL1RA, but rather enhanced it (Fig. 3C and D; $P < 0.05$).

To test if release of IL1RA in response to bleomycin is a consequence of genotoxic stress, we inhibited the ensuing activation of the DDR. Chemical inhibition of ATM (ataxia telangiectasia, mutated) impaired the release of IL1RA (Fig. 3E and F). Together, these observations suggest that IL1RA is released via DDR-dependent nonclassical secretion pathways in response to bleomycin.

Bleomycin induces apoptosis of fibroblasts and cancer cells

To investigate if the release of IL1RA in response to bleomycin was a consequence of DDR-mediated apoptosis, we measured early- and late-stage events of apoptosis. Early apoptosis was measured by examining the binding of Annexin V to translocated phosphatidylserine on bleomycin-treated cells. Uptake of 7-amino-actinomycin D (7-AAD) by cells was used to analyze the loss of cell membrane integrity at the late stage of apoptosis. In response to bleomycin treatment, early- and late-stage events of apoptosis appeared after 8 hours of treatment with bleomycin, and the percentage of apoptotic cells increased further over the next 40 hours (Fig. 4A; $P < 0.05$). The loss of the mitochondrial membrane potential in response to DNA damage can promote the activation of caspase 9 and caspase 8 (27). Caspase 9 cleaves and activates caspase 3 and caspase 7 leading to apoptosis of cells. In accordance, the activation of caspase 9, caspase 7, and

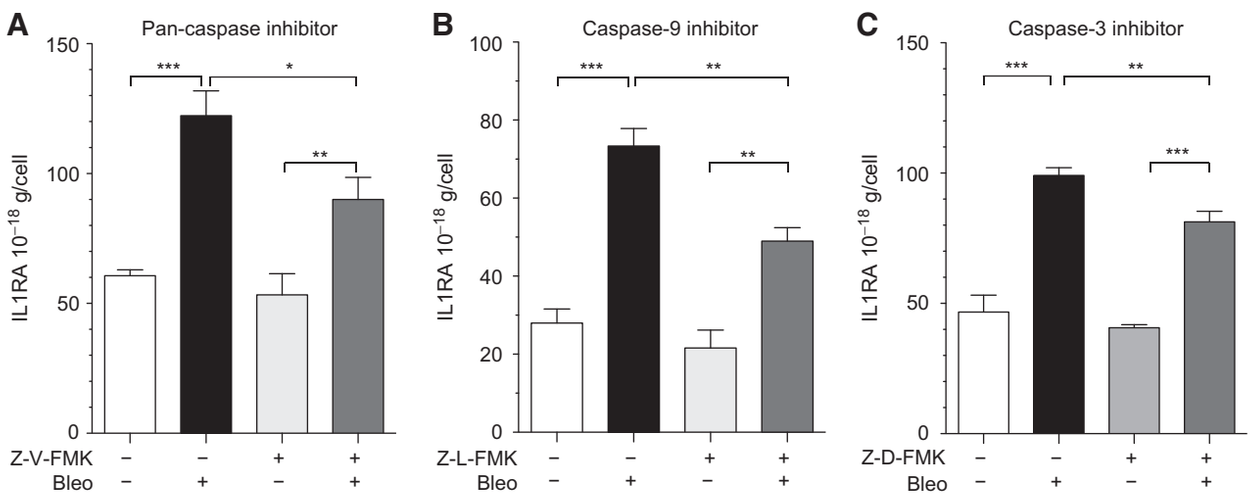

Figure 5.
Release of IL1RA in response to DNA damage is regulated by caspase 9 and caspase 3. A–C, primary fibroblasts were pretreated for 1 hour with 20 μmol/L of the general caspase inhibitor Z-VAD-FMK (A), 10 μmol/L of the caspase-9 inhibitor Z-LEHD-FMK (B), or 10 μmol/L of the caspase-3 inhibitor Z-DEVD-FMK (C) followed by 30 μg/mL of bleomycin or vehicle for 20 hours. The amount of IL1RA in the supernatant of treated cells was analyzed by ELISA. Results are expressed as mean ± SD of one of at least two independent experiments done in triplicates. *, $P < 0.05$; **, $P < 0.01$; ***, $P < 0.001$.

caspase 3 significantly increased after 4 hours ($P < 0.01$) of bleomycin treatment (Fig. 4B–D). A significant increase in caspase-8 activity was only observed after 16 hours of bleomycin treatment (Fig. 4C; $P < 0.05$). Bleomycin treatment also increased the percentage of apoptotic cancer cells that release IL1RA in response to genotoxic stress (Fig. 4E). In summary, our data show that the rate of apoptosis and the extracellular concentrations IL1RA correlate in response to treatment with bleomycin.

Release of IL1RA depends on caspase 9 and caspase 3

To test the role of caspases in the release of IL1RA in response to bleomycin, we blocked caspase activity prior to treatment of fibroblasts with bleomycin. Chemical inhibition of caspases using the general caspase inhibitor Z-VAD-FMK impaired the release of IL1RA in response to bleomycin (Fig. 5A; $P < 0.05$). Similarly, pretreatment with the irreversible caspase-9 inhibitor Z-LEHD-FMK or the caspase-3 inhibitor Z-DEVD-FMK reduced the release of IL1RA in response to bleomycin (Fig. 5B and C; $P < 0.01$). Collectively, our results demonstrate that bleomycin-induced release of IL1RA partially depends on caspase-9 and caspase 3–mediated apoptosis.

IL1RA released in response to bleomycin impairs IL1 signaling

To investigate if the amounts of IL1RA released in response to bleomycin inhibit IL1-induced upregulation of *IL6* transcripts (Fig. 6A), the supernatant of bleomycin and mock-treated fibroblasts was transferred to a new set of fibroblasts, which were subsequently treated with IL1α. Supernatant from bleomycin-treated fibroblast cultures impaired the IL1-induced upregulation of *IL6* transcripts when compared with supernatant from mock-treated fibroblasts (Fig. 6A; $P < 0.001$). The inhibitory effect of the supernatant from bleomycin-treated fibroblasts depended on IL1RA, as transfer of supernatant from bleomycin-treated *IL1RA*$^{-/-}$ fibroblasts failed to inhibit the upregulation of *IL6* transcripts in response to IL1α (Fig. 6B). Similarly, IL1RA from bleomycin-treated fibroblast cultures impaired the IL1-induced upregulation of *IL6* transcripts in J774.2 cells transfected with poly (dA:dT), an inflammasome inducer (Fig. 6C). Hence, our data show that IL1RA released in response to DNA damage is able to antagonize the binding of IL1 to the IL1R.

Discussion

Intracellular IL1α is constitutively present in the cytosol of many cells (6). During apoptosis, cytosolic IL1α translocates to the nucleus and binds to chromatin (9). IL1α bound to chromatin fails to promote inflammation. In addition, phagocytosis of apoptotic cells by macrophages and immature dendritic cells is associated with reduced secretion of IL1 (4, 28). Here, we show that caspase-mediated apoptosis in response to DNA damage leads to the release of biologic significant amounts of IL1RA. The IL1RA is an important negative regulator of inflammatory responses (10). IL1RA exists as a secreted isoform (sIL1RA) and intracellular isoforms (icIL1RA). The secreted isoform is primarily produced by monocytes and macrophages. *sIL1ra* is the only

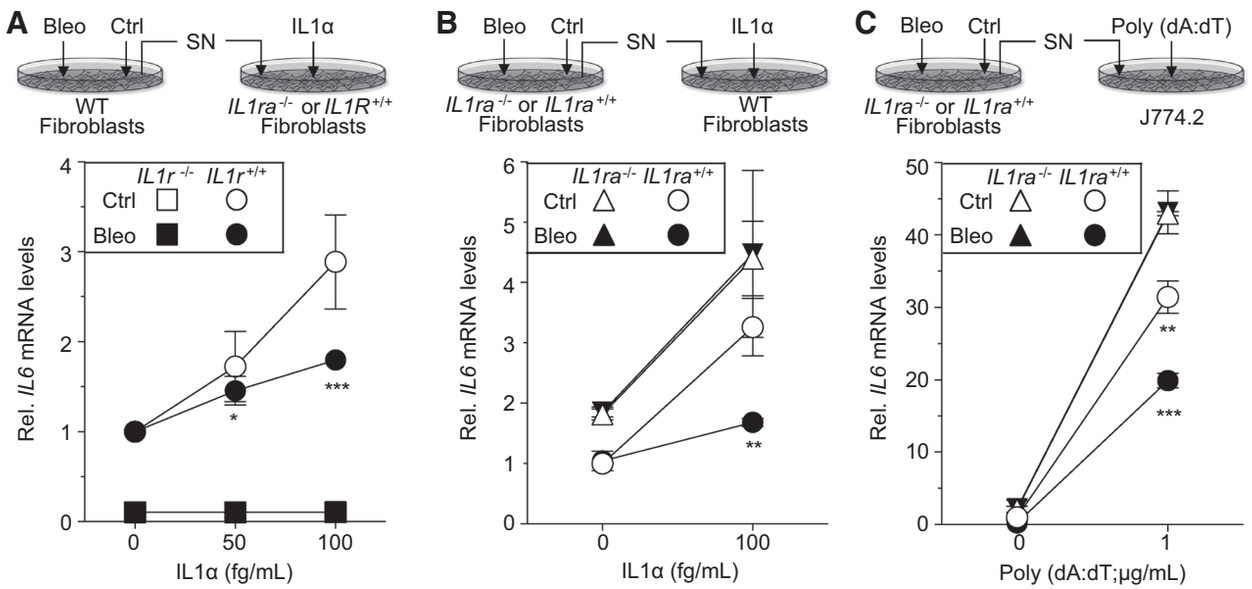

Figure 6.

IL1RA released in response to bleomycin antagonizes IL1R signaling. A, supernatant (SN) of primary fibroblasts treated with 30 μg/mL of bleomycin (bleo; black symbols) or vehicle (ctrl, white symbols) was collected after 20 hours of treatment and transferred to a new set of *IL1r*$^{+/+}$ (round symbols) and *IL1r*$^{-/-}$ (square symbols) fibroblasts. After incubation with the supernatant for 1 hour, the new set of fibroblasts was treated with recombinant IL1α at the indicated concentrations or vehicle for 6 hours. The relative amounts of *IL6* transcripts were determined by qRT-PCR, and the data were normalized to vehicle-treated *IL1r*$^{+/+}$ fibroblast samples. B, supernatant of *IL1ra*$^{+/+}$ (round symbols) and *IL1ra*$^{-/-}$ (triangular symbols) fibroblasts treated with 30 μg/mL bleomycin (black symbols) or vehicle (white symbols) was collected after 20 hours of treatment. The collected supernatant was added to untreated fibroblasts for 1 hour. Subsequently, 100 fg/mL of recombinant IL1α was added for 6 hours, and the relative amounts of *IL6* transcripts were determined by qRT-PCR. The data were normalized to the amounts of *IL6* and *Hprt* transcripts in fibroblasts pretreated with medium only. C, supernatant of *IL1ra*$^{+/+}$ (round symbols) and *IL1ra*$^{-/-}$ (triangular symbols) fibroblasts treated with 30 μg/mL bleomycin (black symbols) or vehicle (white symbols) was collected after 20 hours of treatment. The collected supernatant was added to J774.2 cells transfected overnight with 1 μg/mL of poly (dA:dT) after pretreatment with 1 μmol/L of PMA for 3 hours and subsequent treatment with 2 μg/mL of LPS for 16 hours. The relative amounts of *IL6* transcripts were determined by qRT-PCR as described in B. *, $P < 0.05$; **, $P < 0.01$; ***, $P < 0.001$.

gene in the *IL1ra* family, which encodes a signal peptide required for the secretion via the ER–Golgi complex secretory pathway (29–31). In contrast, icIL1RA is constitutively expressed in the cytoplasm of fibroblasts, keratinocytes, and other cells as a leaderless protein. icIL1RA consists of a number of isoforms generated by alternative splicing and translation initiation. Like its secreted counterpart, icIL1RA functions as an extracellular receptor antagonist of IL1 when released from cells (32). Our data suggest that icIL1RA is released nonclassical secretion pathways in response to bleomycin treatment as inhibitors of the classical endoplasmic secretion pathways or N-glycosylation, which can enhance secretion of proteins, did not abrogate the release of IL1RA (33). It is likely that presynthesized icIL1RA is released by fibroblasts and other cells as *IL1ra* transcripts and intracellular IL1RA levels decreased in response to bleomycin treatment. In addition, *de novo* translation was not required for the bleomycin-induced release of IL1RA. Many IL1 family members lack classical signal sequences necessary for secretion *via* the ER–Golgi complex pathway. These cytokines are released by autophagy, necrotic cells, or poorly defined nonclassical secretion pathways (34). No changes in the expression of the autophagy markers LC3-I, LC3-II, and p62 were observed after treatment with bleomycin (data not shown). Furthermore, pretreatment of fibroblasts with the autophagic sequestration blocker 3-methyladenine did not impair bleomycin-induced IL1RA secretion (data not shown), indicating that the release of IL1RA is not regulated by autophagy. IL1RA concentrations in the supernatant of bleomycin-treated fibroblasts correlated with the percentage of apoptotic but necrotic cells. Furthermore, inhibition of the apoptosis-inducing caspase 9 and caspase 3 impaired the release of IL1RA, supporting the conclusion that IL1RA is released by apoptotic cells.

IL1 contributes to the development of certain human cancers and has been suggested as a potential therapeutic target in human cancers (35, 36). Mutated p53 can sustain IL1β-driven tumor malignancy by suppressing the expression of *IL1RA* (37). p53 is frequently mutated in many different cancers, and mutations of p53 correlate with a decrease in apoptosis in some cancer models (38–40). Hence, our data indicate that the release of IL1RA by apoptotic cells expressing wild-type p53, but not mutated p53, may antagonize a proinflammatory tumor microenvironment promoting tumorigenesis. Consistent with this conclusion, IL1RA released by fibroblasts expressing wild-type p53 in response to bleomycin was able to impair IL1-induced *IL6* expression. However, the tested murine cancer cells were able to release IL1RA in response to bleomycin, suggesting that only certain p53 mutations might be able to suppress the expression of *IL1ra* or that mouse and human *IL1RA* are regulated differentially by p53.

Disclosure of Potential Conflicts of Interest

No potential conflicts of interest were disclosed.

Authors' Contributions

Conception and design: J.Y. Chwee, M. Khatoo, N.Y. Jie Tan, S. Gasser
Development of methodology: J.Y. Chwee, M. Khatoo, N.Y. Jie Tan, S. Gasser
Acquisition of data (provided animals, acquired and managed patients, provided facilities, etc.): J.Y. Chwee
Analysis and interpretation of data (e.g., statistical analysis, biostatistics, computational analysis): J.Y. Chwee, S. Gasser
Writing, review, and/or revision of the manuscript: M. Khatoo, N.Y. Jie Tan, S. Gasser
Administrative, technical, or material support (i.e., reporting or organizing data, constructing databases): S. Gasser
Study supervision: S. Gasser
Other (generated data for Figs. 1A–E, 2A and B, 3B and C, 5: J.Y. Chwee

Acknowledgments

The authors thank Dr. P. Hutchinson for technical assistance in flow cytometry.

Grant Support

This work was supported by Biomedical Research Council grant 07/1/21/19/513 and the National Research Foundation grant Hebrew University of Jerusalem-CREATE—Cellular and Molecular Mechanisms of Inflammation.

The costs of publication of this article were defrayed in part by the payment of page charges. This article must therefore be hereby marked *advertisement* in accordance with 18 U.S.C. Section 1734 solely to indicate this fact.

Received March 28, 2015; revised October 6, 2015; accepted January 4, 2016; published OnlineFirst February 12, 2016.

References

1. van Vugt MA, Bras A, Medema RH. Restarting the cell cycle when the checkpoint comes to a halt. Cancer Res 2005;65:7037–40.
2. Harrison JC, Haber JE. Surviving the breakup: The DNA damage checkpoint. Annu Rev Genet 2006;40:209–35.
3. Bartek J, Lukas J. DNA damage checkpoints: From initiation to recovery or adaptation. Curr Opin Cell Biol 2007;19:238–45.
4. Voll RE, Herrmann M, Roth EA, Stach C, Kalden JR, Girkontaite I. Immunosuppressive effects of apoptotic cells. Nature 1997;390:350–1.
5. Elliott MR, Ravichandran KS. Clearance of apoptotic cells: Implications in health and disease. J Cell Biol 2010;189:1059–70.
6. Garlanda C, Dinarello CA, Mantovani A. The interleukin-1 family: Back to the future. Immunity 2013;39:1003–18.
7. Xue W, Zender L, Miething C, Dickins RA, Hernando E, Krizhanovsky V, et al. Senescence and tumour clearance is triggered by p53 restoration in murine liver carcinomas. Nature 2007;445:656–60.
8. Apte RN, Dotan S, Elkabets M, White MR, Reich E, Carmi Y, et al. The involvement of IL-1 in tumorigenesis, tumor invasiveness, metastasis and tumor-host interactions. Cancer Metastasis Rev 2006;25:387–408.
9. Cohen I, Rider P, Carmi Y, Braiman A, Dotan S, White MR, et al. Differential release of chromatin-bound IL-1alpha discriminates between necrotic and apoptotic cell death by the ability to induce sterile inflammation. Proc Natl Acad Sci U S A 2010;107:2574–9.
10. Dinarello CA. The biological properties of interleukin-1. Eur Cytokine Netw 1994;5:517–31.
11. Aksentijevich I, Masters SL, Ferguson PJ, Dancey P, Frenkel J, van Royen-Kerkhoff A, et al. An autoinflammatory disease with deficiency of the interleukin-1-receptor antagonist. N Engl J Med 2009;360:2426–37.
12. Reddy S, Jia S, Geoffrey R, Lorier R, Suchi M, Broeckel U, et al. An autoinflammatory disease due to homozygous deletion of the IL1RN locus. N Engl J Med 2009;360:2438–44.
13. Arend WP, Palmer G, Gabay C. IL-1, IL-18, and IL-33 families of cytokines. Immunol Rev 2008;223:20–38.
14. Hirsch E, Irikura VM, Paul SM, Hirsh D. Functions of interleukin 1 receptor antagonist in gene knockout and overproducing mice. Proc Natl Acad Sci U S A 1996;93:11008–13.
15. Horai R, Saijo S, Tanioka H, Nakae S, Sudo K, Okahara A, et al. Development of chronic inflammatory arthropathy resembling rheumatoid arthritis in interleukin 1 receptor antagonist-deficient mice. J Exp Med 2000;191:313–20.
16. Ma Y, Thornton S, Boivin GP, Hirsh D, Hirsch R, Hirsch E. Altered susceptibility to collagen-induced arthritis in transgenic mice with aberrant expression of interleukin-1 receptor antagonist. Arthritis Rheum 1998;41:1798–805.

17. Palmer G, Talabot-Ayer D, Kaya G, Gabay C. Type I IL-1 receptor mediates IL-1 and intracellular IL-1 receptor antagonist effects in skin inflammation. J Invest Dermatol 2007;127:1938–46.
18. Nicklin MJ, Hughes DE, Barton JL, Ure JM, Duff GW. Arterial inflammation in mice lacking the interleukin 1 receptor antagonist gene. J Exp Med 2000;191:303–12.
19. Merhi-Soussi F, Kwak BR, Magne D, Chadjichristos C, Berti M, Pelli G, et al. Interleukin-1 plays a major role in vascular inflammation and atherosclerosis in male apolipoprotein E-knockout mice. Cardiovasc Res 2005; 66:583–93.
20. Arend WP, Guthridge CJ. Biological role of interleukin 1 receptor antagonist isoforms. Ann Rheumat Dis 2000;1:i60–4.
21. Yoon GS, Sud S, Keswani RK, Baik J, Standiford TJ, Stringer KA, et al. Phagocytosed clofazimine biocrystals can modulate innate immune signaling by inhibiting TNFalpha and boosting IL-1RA secretion. Mol Pharm 2015;12:2517–27.
22. Craciun LI, DiGiambattista M, Laub R, Goldman M, Dupont E. Apoptosis: A target for potentiation of UV-induced IL-1Ra synthesis by IVIg. Immunol Lett 2007;110:36–41.
23. Craciun LI, Stordeur P, Schandene L, Duvillier H, Bron D, Lambermont M, et al. Increased production of interleukin-10 and interleukin-1 receptor antagonist after extracorporeal photochemotherapy in chronic graft-versus-host disease. Transplantation 2002;74:995–1000.
24. Madeo F, Herker E, Maldener C, Wissing S, Lachelt S, Herlan M, et al. A caspase-related protease regulates apoptosis in yeast. Mol Cell 2002; 9:911–7.
25. Orjalo AV, Bhaumik D, Gengler BK, Scott GK, Campisi J. Cell surface-bound IL-1alpha is an upstream regulator of the senescence-associated IL-6/IL-8 cytokine network. Proc Natl Acad Sci U S A 2009; 106:17031–6.
26. Molinari M. N-glycan structure dictates extension of protein folding or onset of disposal. Nat Chem Biol 2007;3:313–20.
27. Eisenberg SP, Brewer MT, Verderber E, Heimdal P, Brandhuber BJ, Thompson RC. Interleukin 1 receptor antagonist is a member of the interleukin 1 gene family: Evolution of a cytokine control mechanism. Proc Natl Acad Sci U S A 1991;88:5232–6.
28. Tesniere A, Panaretakis T, Kepp O, Apetoh L, Ghiringhelli F, Zitvogel L, et al. Molecular characteristics of immunogenic cancer cell death. Cell Death Differ 2008;15:3–12.
29. Eisenberg SP, Evans RJ, Arend WP, Verderber E, Brewer MT, Hannum CH, et al. Primary structure and functional expression from complementary DNA of a human interleukin-1 receptor antagonist. Nature 1990;343:341–6.
30. Hannum CH, Wilcox CJ, Arend WP, Joslin FG, Dripps DJ, Heimdal PL, et al. Interleukin-1 receptor antagonist activity of a human interleukin-1 inhibitor. Nature 1990;343:336–40.
31. Corradi A, Bajetto A, Cozzolino F, Rubartelli A. Production and secretion of interleukin 1 receptor antagonist in monocytes and keratinocytes. Cytotechnology 1993;11:S50–2.
32. Zamzami N, Marchetti P, Castedo M, Zanin C, Vayssiere JL, Petit PX, et al. Reduction in mitochondrial potential constitutes an early irreversible step of programmed lymphocyte death in vivo. J Exp Med 1995;181:1661–72.
33. Zhao W, Hu Z. The enigmatic processing and secretion of interleukin-33. Cell Mol Immunol 2010;7:260–2.
34. Han KS, Kim SI, Choi SI, Seong BL. N-Glycosylation of secretion enhancer peptide as influencing factor for the secretion of target proteins from Saccharomyces cerevisiae. Biochem Biophys Res Commun 2005;337: 557–62.
35. Dinarello CA, Simon A, van der Meer JW. Treating inflammation by blocking interleukin-1 in a broad spectrum of diseases. Nat Rev Drug Discov 2012;11:633–52.
36. Dinarello CA. Why not treat human cancer with interleukin-1 blockade? Cancer Metastasis Rev 2010;29:317–29.
37. Ubertini V, Norelli G, D'Arcangelo D, Gurtner A, Cesareo E, Baldari S, et al. Mutant p53 gains new function in promoting inflammatory signals by repression of the secreted interleukin-1 receptor antagonist. Oncogene 2015;34:2493–504.
38. Muller PA, Vousden KH. Mutant p53 in cancer: New functions and therapeutic opportunities. Cancer Cell 2014;25:304–17.
39. Powell E, Piwnica-Worms D, Piwnica-Worms H. Contribution of p53 to metastasis. Cancer Discov 2014;4:405–14.
40. Attardi LD, Jacks T. The role of p53 in tumour suppression: lessons from mouse models. Cell Mol Life Sci 1999;55:48–63.